

# EFFECT OF INTERMEDIATE ZRO<sub>2</sub>-CAO COATINGS DEPOSITED BY COLD THERMAL SPRAYING ON THE TITANIUM-PORCELAIN BOND IN DENTAL RESTORATIONS

**Emanuela Marcelli, PhD,<sup>a</sup> Maria Laura Costantino, PhD,<sup>b</sup> Tomaso Villa, PhD,<sup>c</sup> Paola Bagnoli, PhD,<sup>d</sup> Romano Zannoli, PhD,<sup>e</sup> Ivan Corazza, PhD,<sup>f</sup> and Laura Cercenelli, PhD<sup>g</sup>**  
University of Bologna, Bologna, Italy; Polytechnic University of Milan, Milan, Italy; IRCCS Galeazzi Orthopaedic Institute, Milan, Italy

<sup>a</sup>Associate Professor, Experimental Diagnostic and Specialty Medicine Department, University of Bologna.

<sup>b</sup>Full Professor, Laboratory of Biological Structure Mechanics, Department of Chemistry, Materials and Chemical Engineering "Giulio Natta," Polytechnic University of Milan.

<sup>c</sup>Assistant Professor, Laboratory of Biological Structure Mechanics, Department of Chemistry, Materials and Chemical Engineering "Giulio Natta," Polytechnic University of Milan; Istituti di Ricovero e Cura a Carattere Scientifico, Istituto Ortopedico Galeazzi.

<sup>d</sup>Postdoctoral Fellow, Laboratory of Biological Structure Mechanics, Department of Chemistry, Materials and Chemical Engineering "Giulio Natta," Polytechnic University of Milan.

<sup>e</sup>Full Professor, Experimental Diagnostic and Specialty Medicine Department, University of Bologna.

<sup>f</sup>Assistant Professor, Experimental Diagnostic and Specialty Medicine Department, University of Bologna.

<sup>g</sup>Postdoctoral Fellow, Experimental Diagnostic and Specialty Medicine Department, University of Bologna.

Titanium (Ti) has become popular as a substrate material for Metal ceramic restorations in dentistry because of properties such as low density, low cost, high strength comparable with that of stainless steel, corrosion resistance, and excellent biocompatibility.<sup>1</sup> The clinical performance of Ti in metal ceramic restorations has been evaluated in several studies.<sup>2-6</sup> The chemical bond between the Ti substrate and the ceramic veneer is achieved through the porcelain firing process. However, the formation of a poorly adhering oxide on Ti at dental porcelain sintering temperatures causes adherence problems at the interface between Ti and porcelain, the main limiting factor in the fabrication of Ti ceramic restorations.<sup>7-12</sup> Another possible source of Ti-porcelain bond failure is the stress caused by the mismatch of the thermal expansion coefficient of Ti and ceramic, which may affect the flexural bond strength of the Ti ceramic system.<sup>13</sup>

Several studies have been carried out to improve the bond strength of Ti-ceramic systems with procedures that involve the use of bonding agents<sup>14-18</sup> or surface modification on the Ti substrate before porcelain application.<sup>17,19-23</sup> Bonding agents contain a mixture of Ti and ceramic particles that may reduce the thermal expansion mismatch between the metal and the ceramic material.<sup>15</sup> However, some researchers report that the excessive thickness and the composition of the bonding agents may strongly affect the resulting metal-ceramic bond.<sup>14,16</sup> Ti surface treatments may limit the

formation of the deleterious oxide layer on Ti at elevated temperatures. A roughened surface by airborne-particle abrasion enables mechanical interlocking and provides an increased surface for bonding metal and ceramics.<sup>14,17,18,24-26</sup> Wang and Fung<sup>27</sup> deposited a chromium coating layer by physical vapor deposition sputtering on the Ti substrate before porcelain veneering.

In other studies,<sup>28,29</sup> a gold-sputtered coating layer was applied. Researchers also reported the use of different kinds of protective ceramic coatings to enhance the Ti-porcelain bond strength.<sup>30-32</sup> Zirconia ( $ZrO_2$ ) ceramics and their compounds play an exceptional role among the ceramic materials used for this purpose.<sup>33</sup>  $ZrO_2$  exhibits 3 temperature-dependent polymorphs: monoclinic, tetragonal, and cubic. To avoid the phase transformation from monoclinic to tetragonal during high-temperature exposure, the high-temperature tetragonal and cubic phases of  $ZrO_2$  can be stabilized at room temperature by the aliovalent substitution of lower valent oxides, such as calcium oxide (CaO), magnesium oxide (MgO), or yttrium oxide ( $Y_2O_3$ ).<sup>34</sup> Cubic  $ZrO_2$  stabilized with 8 wt%  $Y_2O_3$  is the most widely proposed compound for ceramic coatings intended to enhance the Ti-porcelain bond strength in dentistry.<sup>33,35,36</sup> As in aerospace gas turbine engines, it provides the best performance in high-temperature applications experienced in the field of thermal barrier coatings,<sup>34</sup> which are ceramic coatings used to protect and

insulate metallic components exposed to high temperatures.  $ZrO_2$  stabilized by CaO and MgO also has been studied for thermal barrier coatings<sup>34</sup> and might be a viable compound for producing protective coating layers and promoting adhesion in Ti-ceramic dental restorations. In spite of the technologic improvements that have been made in ceramic veneering on the Ti substrate and in the methods and materials proposed for altering the Ti surface, further investigation is required to improve Ti-porcelain bonding mechanisms and to further implement the use of Ti-ceramic restorations in clinical practice.<sup>37,38</sup>

The purpose of this study was to evaluate the effect on the Ti-porcelain bonding of 2 different calcium oxide-stabilized zirconia ( $ZrO_2$ -CaO) coatings deposited on the Ti substrate before porcelain application by using an oxyacetylene cold thermal spraying (ocTS) process. The 2  $ZrO_2$ -CaO coatings were evaluated and compared with a traditional bonder-based technique (control group) that uses a ceramic bonding agent at the Ti-porcelain interface. The bond strengths for the 2 experimental  $ZrO_2$ -based coatings and for the control group were determined with a 3-point bend test. Scanning electron microscopy (SEM) and energy dispersion spectroscopy (EDS) were used to provide the interfacial characterization of the experimental groups and to study the elemental distribution in the debonded areas. The null hypothesis of the study was that the experimental  $ZrO_2$ -CaO coatings would not improve the Ti-porcelain bonding.

**TABLE I.** Groups subjected to debonding tests

| Type    | Description   |
|---------|---|
| Control | Bonder (traditional adhesive technique)                           |
| 1       | ZrO <sub>2</sub> -CaO (deposition by ocTS)                        |
| 2       | ZrO <sub>2</sub> -CaO + bond coat (Ni-Al-Mo) (deposition by ocTS) |

ZrO<sub>2</sub>-CaO, calcium oxide-stabilized zirconia; ocTS, oxyacetylene cold thermal spraying; Ni, nickel; Al, aluminum; Mo, molybdenum.

**TABLE II.** Firing procedures used for bonder-based technique (control)

| Parameter             | Bonder                  | Opaque                  | Dentin                  | Glaze |
|-----------------------|-------------------------|-------------------------|-------------------------|-------|
| Base temperature, °C  | 500                     | 500                     | 500                     | 500   |
| Drying time, min      | 6                       | 4                       | 6                       | 2     |
| Heat rate, °C/min     | 65                      | 65                      | 55                      | 55    |
| Vacuum start, °C      | 500                     | 500                     | 500                     | —     |
| Vacuum end, °C        | 795                     | 795                     | 755                     | —     |
| Final temperature, °C | 795                     | 795                     | 755                     | 755   |
| Holding time, min     | 1 min<br>(under vacuum) | 1 min<br>(under vacuum) | 1 min<br>(under vacuum) | 1 min |

From manufacturer's processing instructions (Dentaurum Inc).

**TABLE III.** Oxyacetylene cold thermal spraying parameters\*

| Parameter                                | Value |
|--|-------|
| Acetylene pressure, MPa                  | 0.07  |
| Oxygen pressure, MPa                     | 0.4   |
| Air pressure, MPa                        | 0.1   |
| Spraying speed, m/min                    | 25    |
| Burner distance from sprayed surface, mm | 150   |
| No. applied layers                       | 6     |

\*Firing procedures are from manufacturer's processing instructions (Castolin Eutectic Group).

## MATERIAL AND METHODS

### Debonding tests

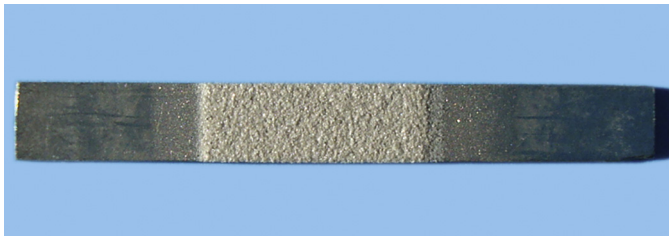
Debonding tests were performed according to the International Organization of Standardization (ISO) 9693-1:2012 standard,<sup>39</sup> which specifies procedures for characterizing the debonding strength ( $T_{deb}$ ) of metal-ceramic dental restorations. By following the requirements of the ISO 9693-1:2012

standard,<sup>39</sup> the specimens were rectangular bars (length=25 ±1 mm, width=3.0 ±0.1 mm, height=0.50 ±0.05 mm) of commercially pure Ti (TiWL.3.7034, grade 2; Titanium International Group Srl) used as the substrate metal for the overlying porcelain layer (opaque and dentin, TRICERAM; Dentaurum Inc). Ti bars were airborne-particle abraded with alumina particles (size, 100-150 μm) and ultrasonically cleaned in acetone for 10 minutes. They then were divided into 3 groups of 12 specimens each (Table I). The control group was prepared by following the traditional adhesive technique that uses a bonding agent at the Ti-ceramic interface. A paste bonder (TRICERAM Bonder; Dentaurum Inc) was applied thinly onto the Ti substrate with a glass spatula and avoiding the formation of puddles or drops. The opaque was applied in a thin even layer on the bonder-covered framework, taking care to cover the entire surface; subsequently, dentin and glaze firings were carried out (Table II).

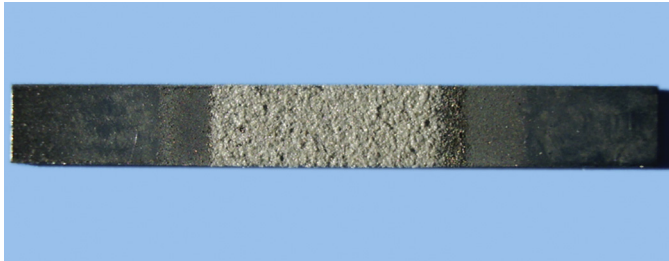
The 2 experimental groups (types 1 and 2) received coatings of ZrO<sub>2</sub>-CaO

(70 wt% ZrO<sub>2</sub> stabilized with 30 wt% CaO) powders (MetaCeram 28085; Castolin Eutectic Group) applied with an ocTS system (CastoDyn DS 8000 torch; Castolin Eutectic Group) before applying the standard porcelain layer (opaque and dentin) and firing procedures. Type 1 coating was obtained by directly spraying ZrO<sub>2</sub>-CaO powders with the ocTS system, whereas type 2 coating was produced by spraying a bond coat of nickel (Ni), 6 aluminum (Al), 5 molybdenum (Mo) (wt%) alloy (RotoTec 51000; Castolin Eutectic Group) before spraying with ZrO<sub>2</sub>-CaO powders.

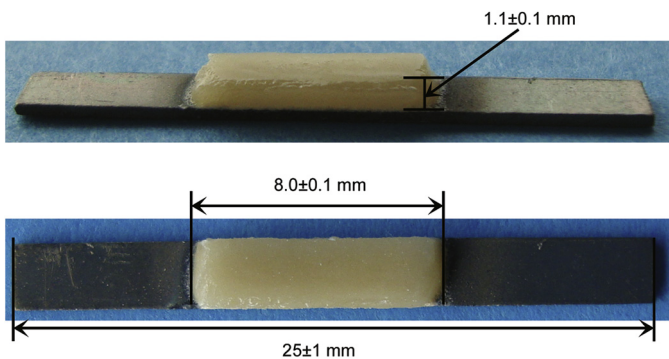
The parameters applied for the ocTS process are reported in Table III. The mean ±SD thickness obtained for the experimental coatings was 103 ±5 μm, which was verified with a micrometer (0-25 mm; Borletti Measuring and Control Instruments). Photographs of types 1 and 2 coatings are found in Figures 1 and 2. For all the tested specimens, uniform layers of opaque and dentin were applied to the central portion of each metal bar to build up a porcelain layer of 8.0×3.0×1.1 mm according to the ISO 9693-1:2012 standard<sup>39</sup> (Fig. 3). All debonding tests were conducted with a mechanical testing machine (MTS 858 Mini Bionix; MTS Systems) composed of an axial-torsional actuator (±15 kN-150 Nm), a displacement transducer linear variable displacement transducer (±100 mm), an angular transducer angular displacement transducer (±140 degrees), and an axial-torsional load cell (MTS 662.20D-04, S/N 1011239). The specimens were tested in a 3-point bend test bench with a support span of 20 mm (Fig. 4). A center load was applied at a crosshead speed of 1.5 mm/min. For each specimen, the load versus the crosshead displacement curve was registered, and the descending tract (that is, from zero load to load at failure [ $F_{fail}$ ]) of the curve was fitted by using a fourth-degree polynomial equation ( $R^2 > 0.99$ ). The mean curve for each group was calculated from the average of the polynomial interpolation of the



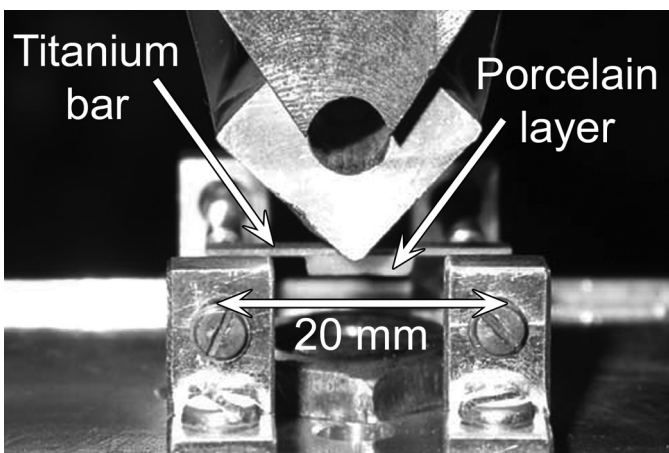
**1** Specimen with type 1 coating:  $ZrO_2$ -CaO deposited by oxyacetylene cold thermal spraying.



**2** Specimen with type 2 coating:  $ZrO_2$ -CaO deposited by oxyacetylene cold thermal spraying in combination with substrate of nickel-aluminum-molybdenum alloy used as bond coat.



**3** Example of definitive specimen of titanium bar with applied coating (type 1) and overlying porcelain layer.



**4** Mechanical testing machine with specimen subjected to debonding test.

experimental curves.<sup>40,41</sup> Metal-ceramic ( $T_{deb}$  [MPa]) for materials loaded in a 3-point flexure test configuration was determined with the following equation:

$$T_{deb} = k \times F_{fail},$$

where the coefficient  $k$  ( $mm^{-2}$ ) is a function of the elastic modulus and thickness of the metal used.<sup>39</sup> The acceptable lower limit for  $T_{deb}$  in a 3-point bend test according to ISO 9693-1:2012 standard<sup>39</sup> is 25 MPa. For each group, 10 specimens were tested, and  $T_{deb}$  data were reported as mean ( $\pm$ standard deviation [SD]) values. The differences in the debond strengths were investigated statistically with 1-way ANOVA ( $\alpha=.05$ ). After the ANOVA results, all possible pairwise comparisons were statistically analyzed with the Student-Newman-Keuls (SNK) test ( $\alpha=.05$ ).

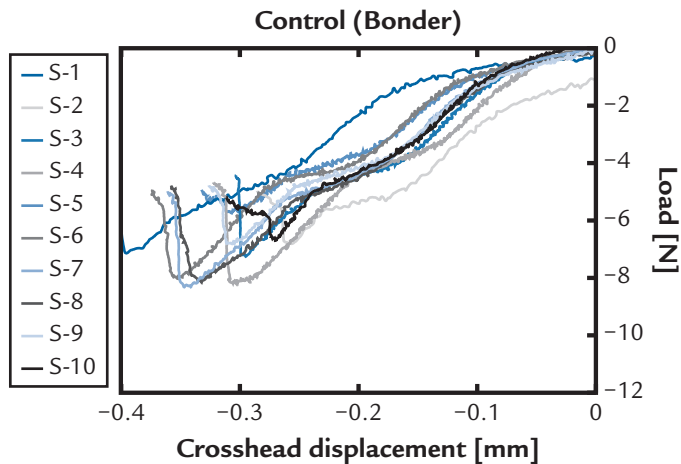
### SEM analysis

The cross-sectional microstructure of the Ti-porcelain interface and the interfacial fractographs of representative debonded specimens in the 3 groups were examined with SEM (EVO 50 EP; Carl ZEISS AG) equipped with an EDS system (INCA Energy 200, LZ4 spectrometer; Carl ZEISS AG). For each group, 2 specimens that were not subjected to debonding tests were used for SEM interfacial characterization of the Ti-porcelain interface. These specimens were embedded in an autopolymerizing acrylic resin and then sectioned in the midsection along their width so that the cross-sectional area could be examined. For each group, SEM micrographs were made of representative areas of the failed surfaces after the 3-point bend test, and EDS mapping was used to study the elemental distribution in the debonded areas (by analyzing the debonded surfaces from both the Ti and the porcelain sides).

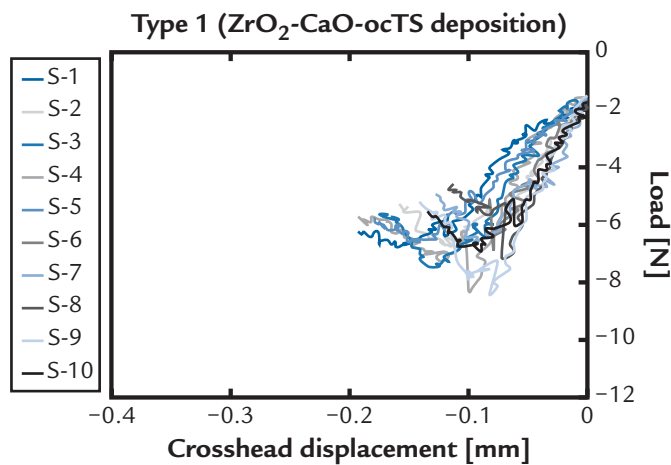
### RESULTS

The load versus crosshead displacement curves obtained from the

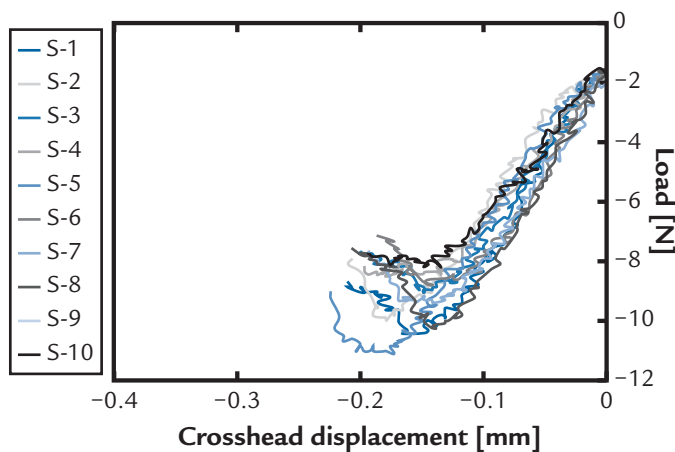
tests are reported in Figures 5 to 7 for all the groups. All the curves have a similar trend characterized by an increasing compressive load as the applied displacement increased until a sudden drop of the load was recorded ( $F_{\text{fail}}$ ), which represents crack initiation in the porcelain versus the Ti interface. The mean curves for all groups are plotted in Figure 8. A lower slope is shown by the control group with respect to the 2 groups treated with  $\text{ZrO}_2$ -based coatings, whereas the highest  $F_{\text{fail}}$  is registered in the type 2 coating. The mean  $T_{\text{deb}}$  collected for all the tested groups are reported in Table IV. Significant differences were found among groups as determined by the 1-way ANOVA ( $F[3,36]=8.6$ ,  $P<.05$ ). The mean ( $\pm\text{SD}$ ) debond strengths for both the control ( $23.51 \pm 2.94$  MPa) and type 1 coating ( $25.97 \pm 2.53$  MPa) were near the acceptable lower limit of 25 MPa.<sup>39</sup> The results from the SNK pairwise comparison test after the significant ANOVA revealed no significant differences between the control group and the  $\text{ZrO}_2$ -CaO powders deposited by ocTS without any preliminary application of a bond coat (type 1 coating). The addition of a substrate of Ni-Al-Mo alloy as a bond coat before applying the  $\text{ZrO}_2$ -CaO powders (type 2 coating) produced an improved Ti-ceramic mean ( $\pm\text{SD}$ ) bonding strength ( $T_{\text{deb}}=39.47 \pm 4.12$  MPa), significantly higher than both the control (SNK test,  $P<.05$ ) and type 1 coating (SNK test,  $P<.05$ ). SEM micrographs of the cross-sectional areas of the specimens not subjected to the bending tests found the presence of an intermediate coating layer of approximately 100  $\mu\text{m}$  in thickness for the type 1 and type 2 groups (Fig. 9B, C). EDS mapping confirmed the composition of these coating layers. For type 2, a substrate of bonding material mainly composed of Ni and Al (Fig. 9C) was evident, whereas, for type 1, the zirconium (Zr) and calcium (Ca) elements were mainly observed (Fig. 9B). Only a Ti phase (substrate) and a ceramic phase (paste bonder and overlaying porcelain layer) were detected for the control group (Fig. 9A). A comparison



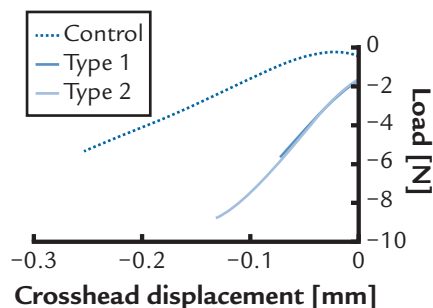
5 Load versus crosshead displacement curves obtained for control group.



6 Load versus crosshead displacement curves obtained for type 1 group.



7 Load versus crosshead displacement curves obtained for type 2 group.



**8** Mean curves of load versus crosshead displacement for each experimental group.

of cross-sectional SEM images of type 1 and type 2 coating layers revealed that type 2 provides a more irregular profile at the interface with the porcelain overlay (Fig. 9C).

SEM micrographs of the debonded Ti surfaces with the associated EDS spectrum and mapping are seen in Figure 10. On the noncoated substrate (control group), minimal residual porcelain was retained, and only a substantial amount of Ti was detected by elemental area analysis, which indicated a substantial adhesive Ti-porcelain bond failure mode (Fig. 10A). The amount of Al content revealed by EDS analysis was probably due to airborne-particle abrasion of the Ti surfaces with alumina particles. The minimal presence of silicon in the debonded Ti surface denotes the lack of bonding agents in the fractured surface. By analyzing the delaminated surface from the porcelain side, a number of elements (silicon, Al, potassium) consistent with the paste bonder composition were identified, together with small Ti remnants. Conversely, a predominant cohesive failure mode was observed for the type 2 group

(Fig. 10C). The debonded surfaces from both the Ti and porcelain sides were mainly covered by elements that belong to the coating material (Ni, Al, Zr, Ca), which thus indicates that the fracture line occurred primarily within the coating layer instead of at the metal-coating or coating-porcelain interfaces. For type 1 coating, the EDS analysis revealed the presence of dark areas that correspond to exposed Ti on the debonded Ti surfaces (Fig. 10B). This may signify a mixed adhesive and cohesive failure mode. Also in this case, the delaminated surface from the porcelain side was substantially covered by elements that compose the coating material (Zr, Ca).

## DISCUSSION

The null hypothesis was rejected based on the study results. Analysis of the results indicate that the bonding strength of porcelain veneered on the Ti substrate is clearly reinforced ( $T_{deb}=39.47$  MPa) by the introduction of a 100- $\mu$ m coating layer of ZrO<sub>2</sub>-CaO powders deposited by ocTS when a bond coat of Ni-Al-Mo alloy is incorporated in the deposition (type 2 coating). The calculated mean curves of load versus crosshead displacement found that type 2 can withstand the maximum load and thus provide a higher  $T_{deb}$  value. SEM micrographs of the debonded surfaces provided further evidence of these results. More specifically, SEM-EDS analysis revealed a substantial cohesive type of failure, which may explain the higher  $T_{deb}$  obtained for type 2. Similarly, SEM analysis reported an adhesive mode of fracture for

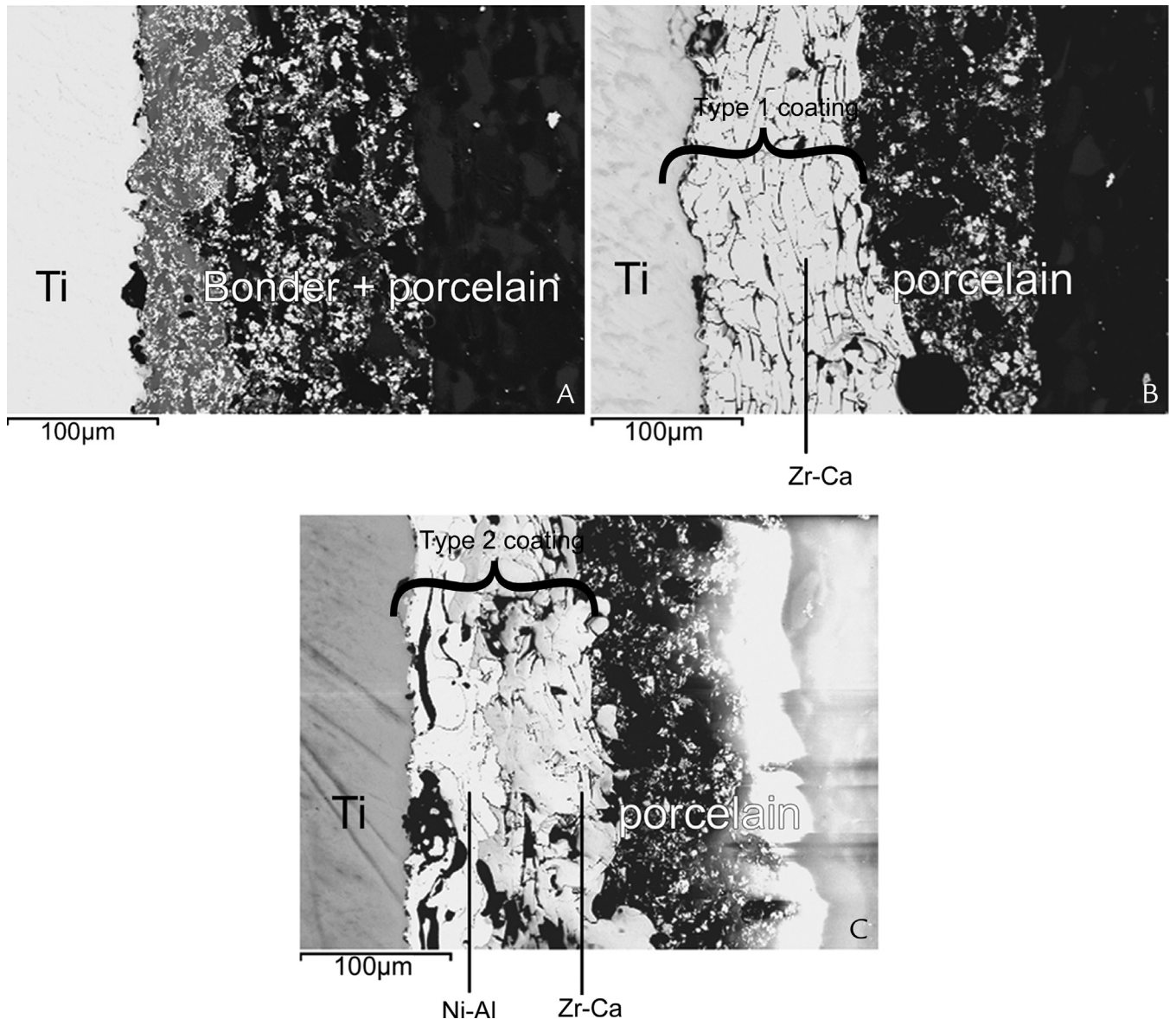
control specimens, which thus confirmed the weaker bond strength obtained from the bending tests. SEM micrographs of the cross section of Ti-porcelain interfaces revealed the presence of Ni and Al (primary composition of the bonding alloy used as bond coat) for type 2. This intermediate Ni aluminide layer that adheres to the Ti substrate probably promoted the reduction of the thermal expansion mismatch between the Ti and the ZrO<sub>2</sub> coating material, which thus improved the overall adhesion. Moreover, the more irregular and indented profile of the interfacial areas between the ZrO<sub>2</sub>-CaO layer and the porcelain may have further promoted interlocking between the surfaces.

Other previous studies proposed the introduction of intermediate ceramic coating layers between the Ti substrate and the porcelain to improve Ti-ceramic adhesion.<sup>14,16,33,42</sup> However, the resulting debond strengths were lower than values obtained in our study. In the study by Derand and Hero,<sup>14</sup> a mean bond strength value of 28 MPa was found when Duceratin ceramic was applied to commercially pure Ti and a protective ZrO<sub>2</sub> layer of 0.5-mm thickness was used on Ti patterns. Mean bond strength values of 27.79 MPa and 32.2 MPa have been given for Noritake Ti22 porcelain when a magnesia investment was used.<sup>16,42</sup> Papadopoulos and Spyropoulos<sup>33</sup> evaluated the effect of submerging Ti patterns in a ceramic slurry of 50 wt% ZrO<sub>2</sub>-Y<sub>2</sub>O<sub>3</sub> and 50 wt% MgO to act as a protective ceramic coating, then investing them with a phosphate-bonded material. The bond strength values obtained for the group that received the ceramic slurry were in the range of 26 to 28 MPa. Lo et al<sup>36</sup> reported that the application of an intermediate plasma-sprayed ZrO<sub>2</sub> layer provides a higher surface roughness, which enhances the mechanical bond at the ZrO<sub>2</sub>-porcelain interface and acts as a sufficient oxygen diffusion barrier at 800°C to prevent the oxidation of Ti at the Ti-ZrO<sub>2</sub> interface. Similarly, Chou and Chang<sup>35</sup> reported that the bonding strength

**TABLE IV.** Results of debonding tests and descriptive statistics according to SNK test

| Type    | No. | $T_{deb}$ (MPa), mean ( $\pm$ SD) | SNK Grouping <sup>a</sup> |
|---------|-----|-----------------------------------|---------------------------|
| Control | 10  | 23.51 $\pm$ 2.94                  | A                         |
| 1       | 10  | 25.97 $\pm$ 2.53                  | A                         |
| 2       | 10  | 39.47 $\pm$ 4.12                  | B                         |

SNK, Student-Newman-Keuls;  $T_{deb}$ , debonding strength; SD, standard deviation.  
<sup>a</sup>Groupings with different letters were significantly different at the .05 level.



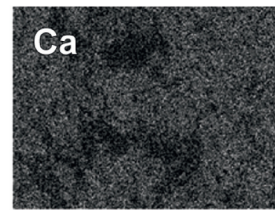
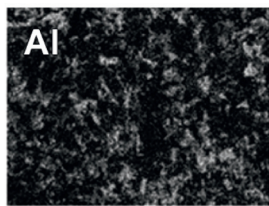
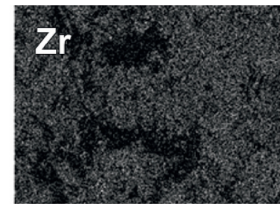
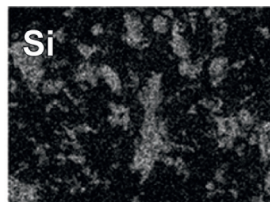
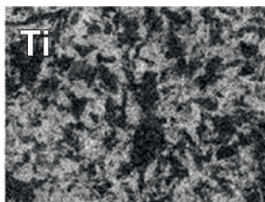
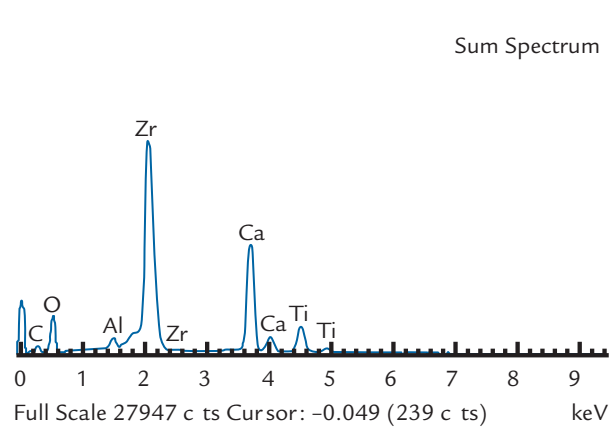
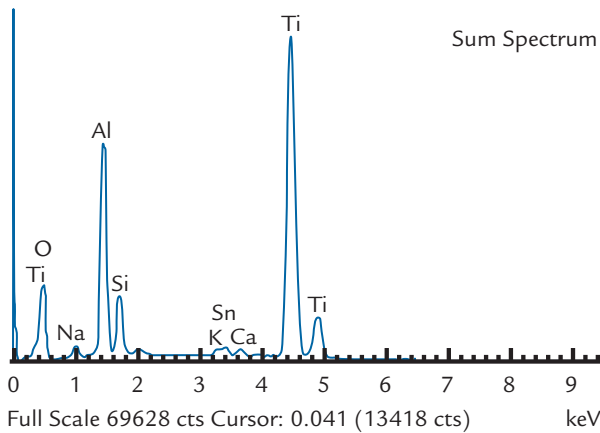
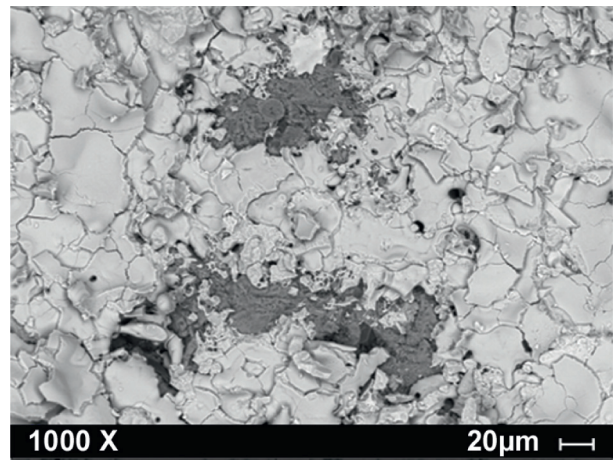
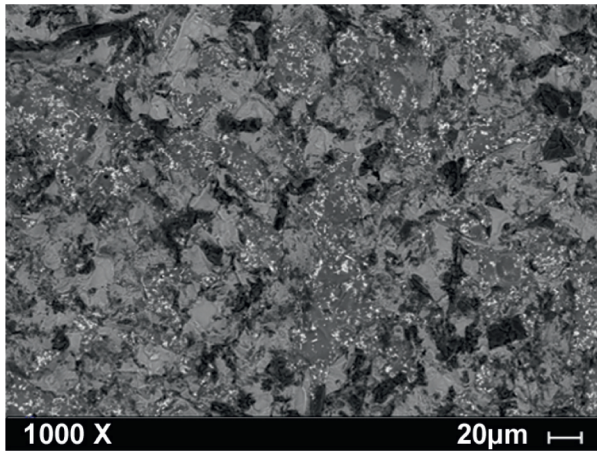
**9** Scanning electron microscopy cross-sectional microstructure of titanium-porcelain interface. A, Control group. B, Type 1 group. C, Type 2 group.

between a Ti substrate and a hydroxyapatite top coating used on metallic implants in orthopedics and dentistry could be increased by introducing a plasma-sprayed  $ZrO_2$  bond coat. Coatings obtained by plasma-spraying (PS) are generally much denser, stronger, and cleaner than those obtained by other thermal spraying processes. However, the PS process itself is complex because of the many interacting process parameters.<sup>43</sup> Also, the cost of the PS process could make it less feasible than a less expensive process that produces almost the same results.

In this study, the 2 experimental  $ZrO_2$ -based coatings differ from the material composition ( $ZrO_2$ -CaO for type 1 and  $ZrO_2$ -CaO+Ni-Al-Mo for type 2), whereas the process of depositing the coatings is the same (namely, ocTS). The ocTS used in this study belongs to the group of flame spraying, which constitutes a well-established technique for producing thermally sprayed coatings.<sup>44</sup> Coatings obtained with flame spraying are available for almost instant use, with no drying or setting time required. The cold variant, especially, involves preheating the substrate up to approximately 100°C and

the deposition of coating, whereas the temperature of the substrate does not exceed 250°C. Thus, the coatings are applied to the desired thickness at temperatures that do not overly stress or change the metal substrate properties or create distortion.

Cold thermal spraying could be particularly practical in dental laboratories because the spraying equipment is inexpensive and easy to handle compared with PS and electron-beam physical vapor deposition. However, analysis of the results of this study indicates that using only  $ZrO_2$ -CaO deposited by ocTS (type 1 coating) leads



A

B

**10** Results of scanning electron microscopy and energy dispersion spectroscopy analysis in representative areas of debonded titanium surfaces. A, Control group. B, Type 1 group. C, Type 2 group.

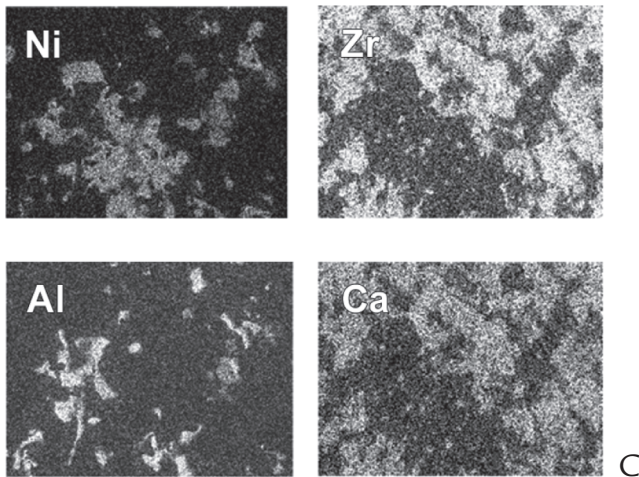
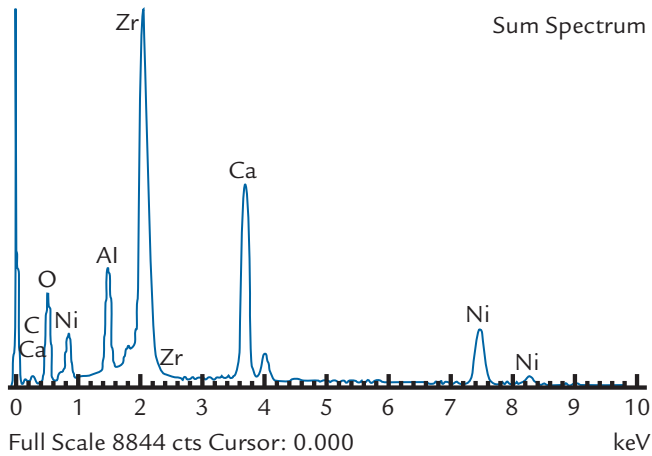
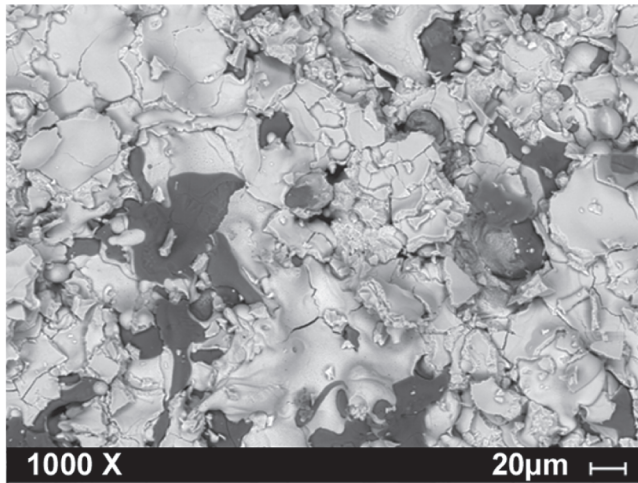
to an unsatisfactory Ti-ceramic bond and produces no significant improvement compared with the control group. A possible explanation for the poor adhesive property of type 1 coating is that, with CaO-stabilized ZrO<sub>2</sub> powders, the coatings include a great number of oxygen ion vacancies, which leads to oxygen transport at high temperatures and to

the formation of a thermally grown oxide layer, which might lead to spallation if an oxidation-resistant bond coat is not provided.<sup>34</sup> Conversely, the ZrO<sub>2</sub>-CaO deposited by ocTS in combination with a bond coat of Ni-Al-Mo alloy (type 2 coating) provides markedly enhanced bond strength. Castolin recommended the Ni-Al-Mo alloy (Rototec 51000) as a

bond coat to be used in combination with ZrO<sub>2</sub>-CaO powder (Metaceram 28085) to produce ceramic coating layers deposited by cold thermal spraying.

Intermetallic, Ni aluminide alloys are widely used as bond coat materials in thermal barrier coatings<sup>45</sup> and have been shown to be highly





**10** (continued) Results of scanning electron microscopy and energy dispersion spectroscopy analysis in representative areas of debonded titanium surfaces. A, Control group. B, Type 1 group. C, Type 2 group.

resistant to oxidation and corrosion, while maintaining structural integrity during thermal cycling. The presence of Al is favorable because the oxidation of Al creates a slow growing and adherent

alumina thermally grown oxide film at the interface, which slows down the oxidation process.<sup>46</sup> However, the use of a Ni-Al-Mo alloy may be undesirable because of the reported Ni sensitivity

in the population.<sup>47,48</sup> Therefore, Ni-free bonding alloys in combination with ZrO<sub>2</sub>-CaO powders should be investigated for use as a bond coat.

Although the 3-point bending test is widely accepted and used to evaluate the metal-ceramic bond strength,<sup>7,8,10,14,16</sup> the mode of failure evaluated in the debonding tests may not directly correspond to the clinical situation. The proposed ZrO<sub>2</sub>-based coatings should be further verified on the irregular surfaces of dental restorations. Hence, future tests with type 2 coating applied on Ti dental crowns and partial fixed dental prostheses before applying the ceramic overlay will be planned to confirm our encouraging preliminary results. Also, the fatigue resistance of these Ti-ceramic systems should be evaluated by exposing them to cyclic loading tests that mimic the physiologic occluding loads and chewing forces that, in the long term, may contribute to Ti-ceramic bonding deterioration.

## CONCLUSION

Within the limits of this study, the following conclusions were drawn. The application on the Ti substrate of a 100- $\mu$ m-thick coating of ZrO<sub>2</sub>-CaO deposited by ocTS in combination with a bond coat of Ni-Al-Mo alloy (type 2 group) produced the most significant improvement in the Ti-ceramic bond strength. The SEM micrographs of the debonded surfaces found a predominant cohesive mode of failure for type 2 specimens, which thus confirmed the highest T<sub>deb</sub> obtained from the debonding tests. The standard bonder-based technique (control group) provided the lowest Ti-ceramic bond strength, very close to the acceptable lower limit of 25 MPa. These findings were confirmed by SEM analysis, which found a substantial adhesive mode of failure at the Ti-porcelain interface. By using only ZrO<sub>2</sub>-CaO deposited by ocTS (type 1 group) produced no significant improvement on the Ti-ceramic bond compared with the standard bonder-based technique, although SEM analysis revealed some mixed adhesive and cohesive modes of failure.

## REFERENCES

1. Wang RR, Fenton A. Titanium for prosthodontics applications: a review of the literature. *Quintessence Int* 1996;27:401-8.
2. Kaus T, Pröbster L, Weber H. Clinical follow-up study of ceramic veneered titanium restorations-three-year results. *Int J Prosthodont* 1996;9:9-15.
3. Chai J, McGivney GP, Munoz CA, Rubenstein JE. A multicenter longitudinal clinical trial of a new system for restorations. *J Prosthet Dent* 1997;77:1-11.
4. Walter M, Reppel PD, Böning K, Freesmeyer WB. Six-year follow-up of titanium and high-gold porcelain-fused-to-metal fixed partial dentures. *J Oral Rehabil* 1999;26:91-6.
5. Lövgren R, Andersson B, Carlsson GE, Odman P. Prospective clinical 5-year study of ceramic-veneered titanium restorations with the Procera system. *J Prosthet Dent* 2000;84:514-21.
6. Hey J, Beuer F, Bense T, Boeckler AF. Metal-ceramic-fixed dental prosthesis with CAD/CAM-fabricated substructures: 6-year clinical results. *Clin Oral Investig* 2013;17:1447-51.
7. Togaya T, Suzuki M, Tsutsumi S, Ida K. An application of pure titanium to the metal porcelain system. *Dent Mater* 1983;2:210-9.
8. Kimura H, Horng CJ, Okazaki M, Takahashi J. Oxidation effects on porcelain-titanium interface reactions and bond strength. *Dent Mater J* 1990;9:91-9.
9. Adachi M, Mackert JR, Parry EE, Fairhurst CW. Oxide adherence and porcelain bonding to titanium and Ti-6Al-4V alloy. *J Dent Res* 1990;69:1230-5.
10. Hautaniemi JA, Hero H, Juhanoja JT. On the bonding of porcelain on titanium. *J Mater Sci* 1992;3:186-91.
11. Yılmaz H, Dincer C. Comparison of the bond compatibility of titanium and an Ni-Cr alloy to dental porcelain. *J Dent* 1999;27:215-22.
12. Kononen M, Kivilahti J. Fusing of dental ceramics to titanium. *J Dent Res* 2001;80:848-54.
13. Low D, Sumii T, Swain M. Thermal expansion coefficient of titanium casting. *J Oral Rehabil* 2001;28:239-42.
14. Derand T, Hero H. Bond strength of porcelain on cast vs. wrought titanium. *Scand J Dent Res* 1992;100:184-8.
15. Gilbert JL, Covey DA, Lautenschlager EP. Bond characteristics of porcelain fused to milled titanium. *Dent Mater J* 1994;10:134-40.
16. Atsu S, Berksun S. Bond strength of three porcelains to two forms of titanium using two firing atmospheres. *J Prosthet Dent* 2000;84:567-74.
17. Reyes MJ, Oshida Y, Andres CJ, Barco T, Hovijitra S, Brown D. Titanium-porcelain system. Part III: effects of surface modification on bond strengths. *Biomed Mater Eng* 2001;11:117-36.
18. Al Hussaini I, Al Wazzan KA. Effect of surface treatment on bond strength of low-fusing porcelain to commercially pure titanium. *J Prosthet Dent* 2005;94:350-6.
19. Jochen DG, Caputo AA, Matyas J. Effect of metal surface treatment on ceramic bond strength. *J Prosthet Dent* 1986;55:186-8.
20. Miyakawa O, Watanabe K, Okawa S, Kanatani M, Nakano S, Kobayashi M. Surface contamination of titanium by abrading treatment. *Dent Mater J* 1996;15:11-21.
21. Hofstede TM, Ercoli C, Graser GN, Tallents RH, Moss ME, Zero DT. Influence of metal surface finishing on porcelain porosity and beam failure loads at the metal-ceramic interface. *J Prosthet Dent* 2000;84:309-17.
22. Troia MG, Henriques GE, Mesquita MF, Fragoso WS. The effect of surface modifications on titanium to enable titanium-porcelain bonding. *Dent Mater* 2008;24:28-33.
23. Zhang CC, Ye JT, Zhang YP, Liao JK, Li BH. Effect of titanium preoxidation on wrought pure titanium to ceramic bond strength. *J Prosthet Dent* 2013;109:106-12.
24. McLean JW, Sced IR. The bonded alumina crown. 1. The bonding of platinum to aluminous dental porcelain using tin oxide coatings. *Aust Dent J* 1976;21:119-27.
25. Anusavice KJ, Phillips RW, Shen C, Rawls HR. Phillips' science of dental materials. 12th ed. St Louis: Elsevier/Saunders; 2013. p. 21-39.
26. Inan O, Acar A, Halkaci S. Effects of sandblasting and electrical discharge machining on porcelain adherence to cast and machined commercially pure titanium. *J Biomed Mater Res B Appl Biomater* 2006;78:393-400.
27. Wang RR, Fung KK. Oxidation behavior of surface modified titanium for titanium-ceramic restorations. *J Prosthet Dent* 1997;77:423-34.
28. Sadeq A, Cai Z, Woody RD, Miller AW. Effects of interfacial variables on ceramic adherence to cast and machined commercially pure titanium. *J Prosthet Dent* 2003;90:10-7.
29. Khung R, Suansuwan NS. Effect of gold sputtering on the adhesion of porcelain to cast and machined titanium. *J Prosthet Dent* 2013;110:101-6.
30. Papadopoulos T, Zinelis S, Vardavoulias M. A metallurgical study of the contamination zone at the surfaces of dental Ti castings, due to the phosphate-bonded investment material: the protection efficacy of a ceramic coating. *J Mater Sci Mater Med* 1999;34:3639-46.
31. Luo XP, Guo TW, Ou YG, Liu Q. Titanium casting into phosphate bonded investment with zirconite. *Dent Mater* 2002;18:512-5.
32. Wang G, Wang X, Zhao Y, Guo T. Effect of a magnetron-sputtered ZrSiN/ZrO<sub>2</sub> film on the bond strength of commercially pure titanium to porcelain. *J Prosthet Dent* 2013;109:313-8.
33. Papadopoulos TD, Spyropoulos KD. The effect of a ceramic coating on the cpTi-porcelain bond strength. *Dent Mater* 2009;25:247-53.
34. Cao XQ, Vassen R, Stoeber D. Ceramic materials for thermal barrier coatings. *J Eur Ceram Soc* 2004;24:1-10.
35. Chou BY, Chang E. Plasma-sprayed zirconia bond coat as an intermediate layer for hydroxyapatite coating on titanium alloy substrate. *J Mater Sci Mater Med* 2002;13:589-95.
36. Lo TN, Chang E, Lui TS. Adherence of porcelain veneered on titanium with an intermediate plasma-sprayed zirconia layer. *Mater Trans* 2004;45:947-52.
37. Mehulic K, Laus-Sosic M. Metal-ceramic bond: how to improve? *Minerva Stomatol* 2009;58:367-73.
38. Haag P, Nilner K. Bonding between titanium and dental porcelain: a systematic review. *Acta Odontol Scand* 2010;68:154-64.
39. International Organization for Standardization. ISO 9693-1:2012. Dentistry—Compatibility testing—Part 1: Metal-ceramic systems. Geneva: ISO; 2012. Available at: [http://www.iso.org/iso/home/store/catalogue\\_tc/catalogue\\_detail.htm?csnumber=54946](http://www.iso.org/iso/home/store/catalogue_tc/catalogue_detail.htm?csnumber=54946). Accessed May 29, 2014.
40. Bagnoli P, Cozzi B, Zaffora A, Acocella F, Fumero R, Costantino ML. Experimental and computational biomechanical characterization of the tracheo-bronchial tree of the bottlenose dolphin (*TURSIOPS TRUNCATUS*) during diving. *J Biomech* 2011;44:1040-5.
41. Bagnoli P, Acocella F, Di Giancamillo M, Fumero R, Costantino ML. Finite element analysis of the mechanical behavior of preterm lamb tracheal bifurcation during total liquid ventilation. *J Biomech* 2013;46:462-9.
42. Yoda M, Konno T, Takada Y, Iijima K, Griggs J, Okuno O, et al. Bond strength of binary titanium alloys to porcelain. *Biomaterials* 2001;22:1675-81.
43. Lugscheider E, Weber T. Plasma spraying: an innovative coating technique: process variants and applications. *IEEE T Plasma Sci* 1990;18:968-73.
44. Katica S. Welding engineering and technology: thermal spraying. In: Slobodan Kralj, editor. *Encyclopedia of life support systems*. Oxford: Eolss Publishers; 2010. p. 1-25.
45. Yu Z, Hass DD, Wadley HNG. NiAl bond coats made by a directed vapor deposition approach. *Mater Sci Eng A* 2005;394:43-52.
46. Feuerstein A, Knapp J, Taylor T, Ashary A, Bolcavage A, Hitchman N. Technical and economical aspects of current thermal barrier coating systems for gas turbine engines by thermal spray and EB-PVD: a review. *Journal of Thermal Spray Technology* 2008;17:199-213.

47. Moffa JP. Biological effects of nickel-containing dental alloys. Council on Dental Materials, Instruments and Equipment. J Am Dent Assoc 1982;104:501-5.
48. Jones TK, Hansen CA, Singer MT, Kessler HP. Dental implications of nickel hypersensitivity. J Prosthet Dent 1996;56:507-9.

**Corresponding author:**

Dr Emanuela Marcelli  
Experimental Diagnostic and Specialty Medicine  
Department  
c/o Policlinico S. Orsola Malpighi  
Via Massarenti 9 (pad.17)  
40138 Bologna  
ITALY  
E-mail: [emanuela.marcelli@unibo.it](mailto:emanuela.marcelli@unibo.it)

**Acknowledgments**

The authors thank Mauro Panfili for technical assistance and Dr Marco Cominetti for use of his dental laboratory for the preparation of the metal-porcelain specimens.